

Simulating Lateral H/He Flame Propagation in Type I X-ray Bursts

Eric T. Johnson¹, Michael Zingale¹

¹Department of Physics and Astronomy, Stony Brook University, Stony Brook, NY 11794-3800 USA

E-mail: eric.t.johnson@stonybrook.edu

Abstract. X-ray bursts are the thermonuclear runaway of a mixed H/He layer on the surface of a neutron star. Observations suggest that the burning begins locally and spreads across the surface of the star as a flame. Recent multidimensional work has looked in detail at pure He flames spreading across a neutron star. Here we report on progress in multidimensional modeling of mixed H/He flames and discuss the challenges.

1. Introduction

Type I X-ray bursts (XRBs) occur in accreting binary systems between a neutron star and a low-mass companion. As a layer of fuel builds up on the surface of the neutron star, gravitational compression heats it up until the conditions at the base lead to a thermonuclear runaway. A challenging aspect of modeling these systems is capturing how the flame spreads from the initial ignition point across the surface of the star. This is important for understanding oscillations observed during the initial rise of some bursts, which are believed to arise from the bright hotspot coming in and out of view as the neutron star rotates [1]. Unfortunately, one-dimensional simulations cannot capture these dynamics, as they are inherently multi-dimensional.

Most burst sources accrete a mix of ^1H and ^4He from a main sequence companion, while some ultra-compact systems accrete nearly pure ^4He [2, 3]. Depending on the accretion rate, the hydrogen can burn stably into helium which will then ignite a pure helium burst, or the helium could ignite before all the hydrogen is consumed, leading to a mixed H/He burst. Previous 2D and 3D simulations by our group and others have been limited to pure helium flames [4–10] as the mixed H/He reaction networks are usually larger and more difficult to integrate, and the timescales are slower due to the weak rate waiting points [11]. We recently showed [10] that the nucleosynthesis and evolution of a spreading flame in 3D matches 2D simulations very closely, so we will focus on 2D simulations here.

2. Simulations

We use the *Castro* [12] compressible hydrodynamics code to perform our simulations, following the simulation methodology developed in [7]. *Castro* uses the AMReX framework [13] for adaptive mesh refinement and parallelization across CPUs and GPUs. We use the stellar equation of state based on [14] and conductivities from [15] for the thermal diffusion operator. *Castro* can use an arbitrary nuclear reaction network, and we discuss some of the options below.

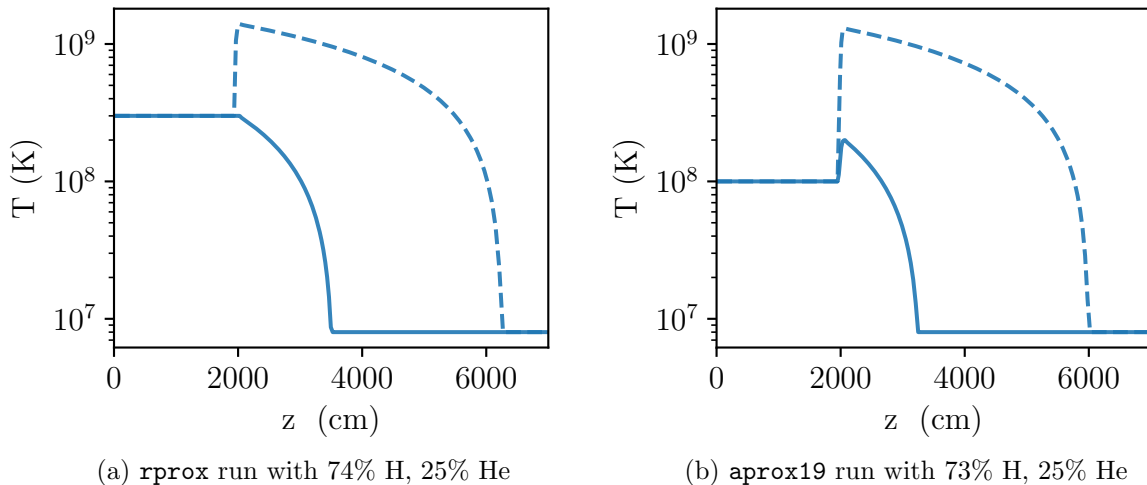


Figure 1: Initial vertical temperature profiles for the cool (solid) and hot (dashed) regions.

All simulations use a two-dimensional axisymmetric simulation domain with a physical size of $2.4576 \times 10^5 \text{ cm} \times 3.072 \times 10^4 \text{ cm}$ and a base grid of 1024×128 zones. The grid is subdivided using two levels of refinement, refining first by a factor of 4, then by a factor of 2. This gives a resolution of 30 cm at the finest level. We note that this is a little coarser than the He simulations we have done previously. However, since the addition of H to the atmosphere increases the scale height and H burning is less strongly peaked than He burning, we believe we can relax the resolution requirements.

Our initial runs used `rprox`, a 10 isotope nuclear reaction network introduced in [16] that models hot CNO burning, triple- α , and rp-process breakout. We vary the proportions of ^1H and ^4He in the fuel layer, and also include 1% of ^{14}O and ^{15}O to help start CNO burning. The oxygen abundance is split between the two isotopes in proportion to their respective β^+ -decay lifetimes. We assume that the composition is completely mixed by a period of convection preceding the ignition of the flame, as explored in [17].

The initial model is set up as described in section 4 of [7]. In summary, it consists of a hot region behind the flame at $T = 1.4 \times 10^9 \text{ K}$ and a cool region ahead of it at $T = 3 \times 10^8 \text{ K}$, with a density of $2 \times 10^6 \text{ g cm}^{-3}$ at the base of the atmosphere ($z = 2000 \text{ cm}$). These two regions are constructed individually in 1D to be in hydrostatic equilibrium vertically, then smoothly blended at the interface, giving us an equilibrium starting condition that will lead to the ignition of a burning front. Figure 1a shows the temperature profiles for the two regions for one of the runs. The other profiles with different compositions are similar, but those with more helium are squashed due to the greater mass of the atmosphere above the surface. The hot region extends to $r_{\text{pert}} = 6.144 \times 10^4 \text{ cm}$ (25% of the domain), and the transition interface between the two regions has a width of $\delta_{\text{blend}} = 2.048 \times 10^3 \text{ cm}$. Paired with the axisymmetric geometry, this effectively models a hotspot at the pole of the star spreading outwards towards the equator. The rotation rate of the neutron star is set to an artificially high 1000 Hz, which helps to confine the flame laterally and allows us to use a smaller simulation domain. All of our simulations were run on the OLCF Summit machine, with the entire calculation offloaded to the NVIDIA V100 GPUs there.

Figure 2 shows snapshots of the mass fraction of ash (everything heavier than ^{16}O) after 80 ms for each of the initial compositions we used. We have found that this diagnostic is much easier to compare between the different compositions than the mean molecular weight, \bar{A} , used in our previous work. The runs in the first two panels never produced well-defined flames. The

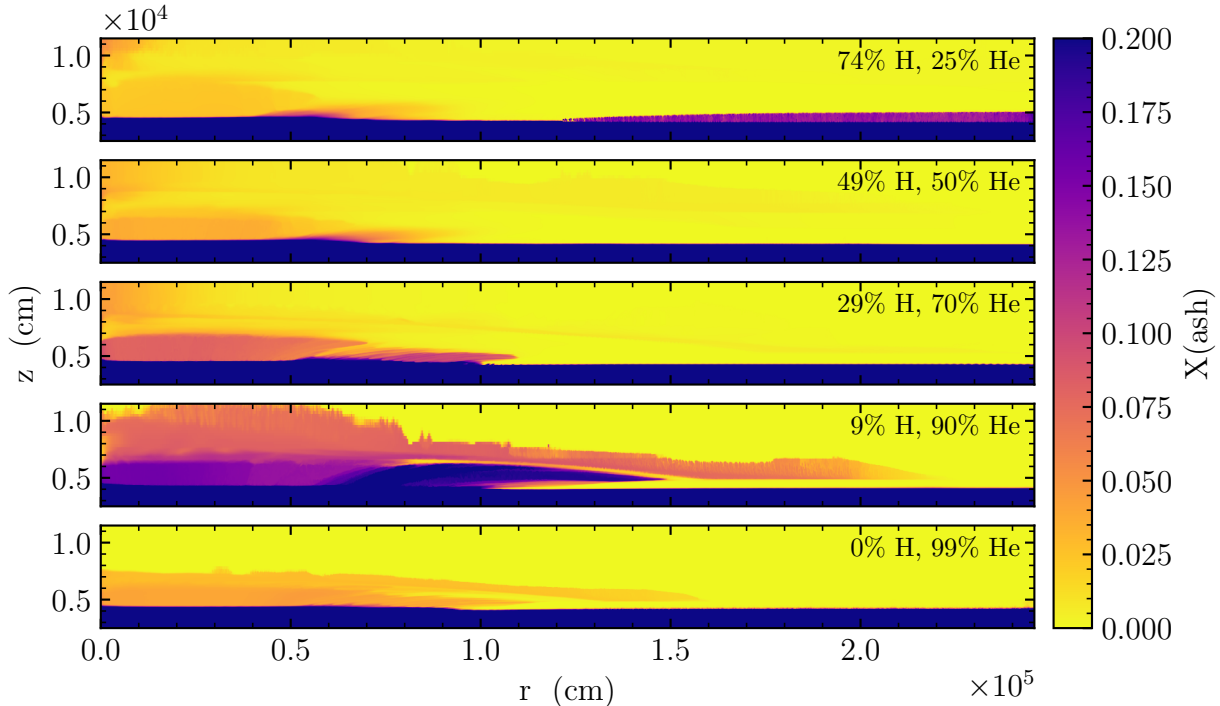


Figure 2: Total mass fraction of all species heavier than ^{16}O for `rprox` runs at $t = 80$ ms.

third panel has more burning than the previous two, but the flame front never moves beyond 10^5 cm. The most interesting is the fourth panel, with 9% H and 90% He, which shows a flame front with burning up to ^{56}Ni . The final panel models a pure He burst using the same network for comparison.

Many of our runs exhibited an unexpected high-temperature region at the base of the atmosphere across the entire simulation domain, starting from the outer radial edge of the domain and spreading toward the pole. This often ignited and consumed all the fuel before the flame could set up and start propagating. The magenta layer on the right of the first panel in figure 2, for example, is a result of this excess burning. We attributed this to our selection of the base temperature in the cool region, and used a lower temperature in later runs to try to avoid this. This is one of the main differences between a pure He burst—a pure He network will not burn much at those temperatures. However, we found that the simulation behavior was very sensitive to any changes in the initial conditions, and it was difficult to reproduce a steady burning front. To explore this behavior in more detail, we experimented with 1D flame simulations using different reaction networks, and found that `aprox19` produced a much more robust propagating flame front than `rprox`. Due to the different composition in that network, we replaced the oxygen isotopes with ^{12}C .

For our next set of runs with `aprox19`, we increased the resolution to 20 cm (using a base grid of 1536×192) and used a new lower boundary condition with a well-balanced pressure reconstruction, as done in [10]. We reduced the cool region temperature to 2×10^8 K and the material below the atmosphere (i.e. the star) to 1×10^8 K, as mentioned above. The new initial conditions are shown in figure 1b. Interestingly, increasing the resolution this way actually scaled slightly better than linear in the number of compute nodes, as the new grid size distributed more evenly onto Summit’s 6 GPUs per node.

Figure 3 shows the same diagnostics as figure 2 for the `aprox19` runs. We can see that the run with 25% He again doesn’t produce a flame, although it does have more ash present in

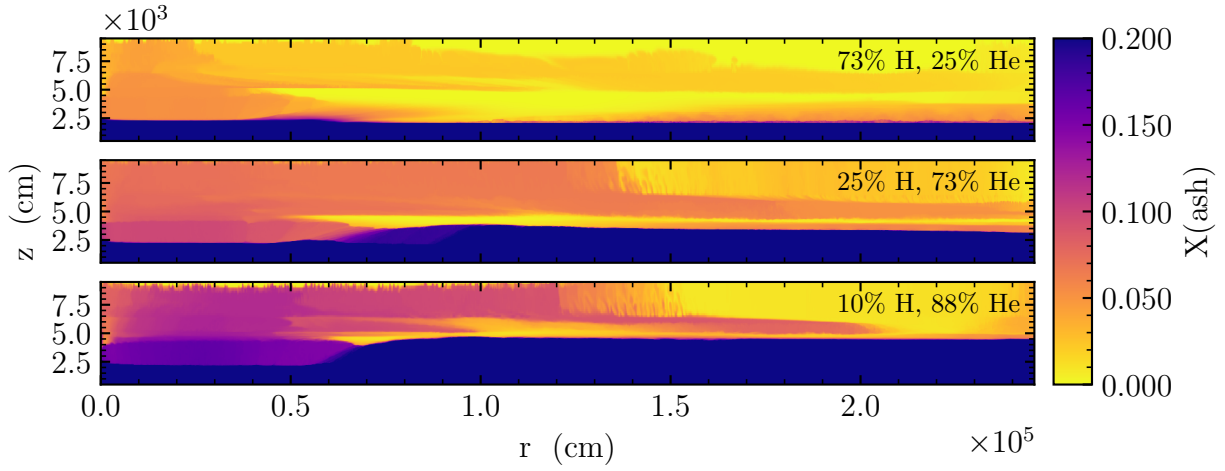


Figure 3: Total ash mass fraction at $t = 80$ ms for `aprox19` runs.

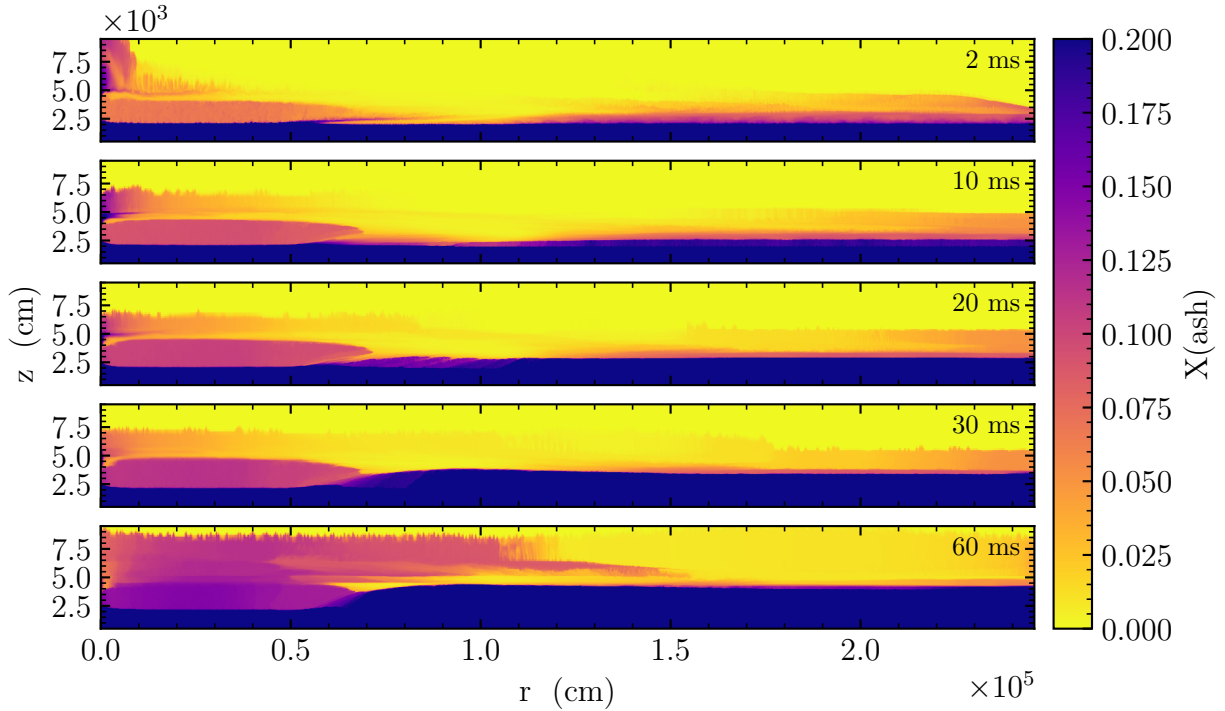


Figure 4: Ash mass fraction evolution for the `aprox19` run with 10% H and 88% He.

the atmosphere than the corresponding `rprox` run. This is due to vigorous carbon burning in the first few milliseconds of the simulation, which consumes the majority of the initial ^{12}C in the lower atmosphere. In other two runs, the right side of the atmosphere heats up and starts burning before the flame front. An example of how this progresses for the run with 10% H and 88% He is shown in figure 4.

Finally, figure 5 shows the evolution of each species in the network over time, for the same run. We can see that most of the initial ^{12}C (solid red line) is consumed in under 1 millisecond. An interesting detail in this plot is the step-like features at early times, most visible in the profiles for ^{28}Si and ^{32}S . These are fairly evenly spaced in time with a separation of $\sim 5 \times 10^{-4}$ s, which matches the width of the domain divided by the average sound speed near the base of the

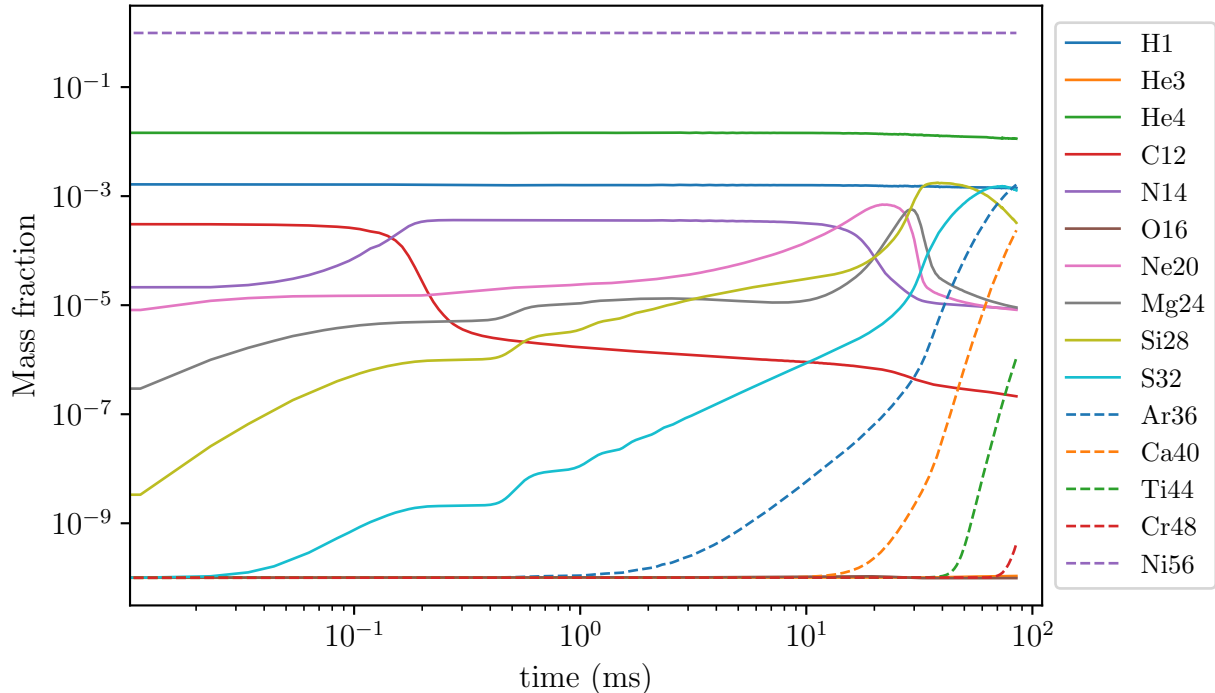


Figure 5: Total mass fractions for each species in the `aprox19` run with 10% H, excluding those which never increased above 10^{-10} .

atmosphere: $L_x/c_s \approx 2.4576 \times 10^5 \text{ cm} / 5.2 \times 10^8 \text{ cm s}^{-1} \approx 4.7 \times 10^{-4} \text{ s}$. This suggests they may be related to acoustic oscillations travelling across the simulation domain and reflecting off of the boundaries.

3. Summary

We ran several two-dimensional simulations of mixed H/He flames in XRBs, varying the proportions of H and He in the atmosphere. We found that the flames are very sensitive to the composition and initial temperatures, which makes it difficult to set up a flame in the first place. Using the `rprox` network, we were only able to produce a stable, propagating flame with an initial composition of 9% H and 90% He. The `aprox19` network gave much better results in 1D simulations, but we have not yet been able to reproduce a clean H/He flame in 2D.

An unexpected hot region would often develop at the surface of the star, away from the flame, which would start burning and disrupt the flame. The source of this heating is unclear, and needs to be investigated further. We are currently testing out different reaction networks with `pynucastro` [18, 19], which allows us to construct and inspect arbitrary reaction networks, and generate C++ code for use in our `Castro` simulations. It also allows us to disable specific rates at runtime, which can help us understand which rates are relevant for H/He burning under these conditions. Finally, we may need to consider different initial models, where the pre-runaway convective mixing is confined only to the He layer at high column depth, as explored in [20].

Acknowledgments

`Castro` is freely available at <http://github.com/AMReX-Astro/Castro>. All of the code and problem setups used here are available in the git repo. The work at Stony Brook was supported by DOE/Office of Nuclear Physics grant DE-FG02-87ER40317. This research used resources of the Oak Ridge Leadership Computing Facility at the Oak Ridge National Laboratory,

which is supported by the Office of Science of the U.S. Department of Energy under Contract No. DE-AC05-00OR22725, awarded through the DOE INCITE program. We thank NVIDIA Corporation for the donation of a Titan X and Titan V GPU through their academic grant program. This research has made use of NASA’s Astrophysics Data System Bibliographic Services.

Software: AMReX [13], Castro [12, 21], GCC (<https://gcc.gnu.org/>), GNU Parallel [22], helmeos [14], linux (<https://www.kernel.org/>), matplotlib [23], NumPy [24, 25], python (<https://www.python.org/>), valgrind [26], VODE [27], yt [28].

References

- [1] Chakraborty M and Bhattacharyya S 2014 *ApJ* **792** 4 ISSN 1538-4357 (*Preprint* 1407.0845) URL <https://doi.org/10.1088/0004-637x/792/1/4>
- [2] Galloway D K and Keek L 2021 *Timing Neutron Stars: Pulsations, Oscillations and Explosions* (*Astrophysics and Space Science Library* vol 461) ed Belloni T M, Méndez M and Zhang C pp 209–262 (*Preprint* 1712.06227)
- [3] in’t Zand J J M, Jonker P G and Markwardt C B 2007 *Astronomy and Astrophysics* **465** 953–963 (*Preprint* astro-ph/0701810)
- [4] Cavecchi Y, Watts A L, Braithwaite J and Levin Y 2013 *Mon. Not. R. Astron. Soc.* **434** 3526–3541 ISSN 0035-8711, 1365-2966 (*Preprint* 1212.2872) URL <https://doi.org/10.1093/mnras/stt1273>
- [5] Cavecchi Y, Watts A L, Levin Y and Braithwaite J 2015 *Mon. Not. R. Astron. Soc.* **448** 445–455 ISSN 1365-2966, 0035-8711 (*Preprint* 1411.2284) URL <https://doi.org/10.1093/mnras/stu2764>
- [6] Cavecchi Y and Spitkovsky A 2019 *ApJ* **882** 142 ISSN 0004-637X, 1538-4357 URL <https://doi.org/10.3847/1538-4357/ab3650>
- [7] Eiden K, Zingale M, Harpole A, Willcox D, Cavecchi Y and Katz M P 2020 *Astrophysical Journal* **894** 6 (*Preprint* 1912.04956)
- [8] Harpole A, Ford N M, Eiden K, Zingale M, Willcox D E, Cavecchi Y and Katz M P 2021 *Astrophysical Journal* **912** 36 (*Preprint* 2102.00051)
- [9] Goodwin A J, Heger A, Chambers F R N, Watts A L and Cavecchi Y 2021 *Monthly Notices of the Royal Astronomical Society* **505** 5530–5542 ISSN 0035-8711 (*Preprint* <https://academic.oup.com/mnras/article-pdf/505/4/5530/38858828/stab1659.pdf>) URL <https://doi.org/10.1093/mnras/stab1659>
- [10] Zingale M, Eiden K and Katz M 2023 *Astrophysical Journal* **952** 160 (*Preprint* 2303.17077) URL <https://dx.doi.org/10.3847/1538-4357/ace04e>
- [11] Strohmayer T and Bildsten L 2006 *Compact Stellar X-ray Sources* ed Lewin W H G and van der Klis M (Cambridge University Press) pp 113–156 URL <https://doi.org/10.1017/cbo9780511536281.004>
- [12] Almgren A S, Beckner V E, Bell J B, Day M S, Howell L H, Joggerst C C, Lijewski M J, Nonaka A, Singer M and Zingale M 2010 *ApJ* **715** 1221–1238 ISSN 0004-637X, 1538-4357 (*Preprint* 1005.0114) URL <https://doi.org/10.1088/0004-637x/715/2/1221>
- [13] Zhang W, Almgren A, Beckner V, Bell J, Blaschke J, Chan C, Day M, Friesen B, Gott K, Graves D, Katz M, Myers A, Nguyen T, Nonaka A, Rosso M, Williams S and Zingale M 2019 *JOSS* **4** 1370 ISSN 2475-9066 URL <https://doi.org/10.21105/joss.01370>
- [14] Timmes F X and Swesty F D 2000 *ASTROPHYS J SUPPL S* **126** 501–516 ISSN 0067-0049, 1538-4365 source code obtained from <http://cococubed.asu.edu/codes/eos.shtml/helmholtz.tbz> URL <https://doi.org/10.1086/313304>

- [15] Timmes F X 2000 *ApJ* **528** 913–945 ISSN 0004-637X, 1538-4357 URL <https://doi.org/10.1086/308203>
- [16] Wallace R K and Woosley S E 1981 *ApJS* **45** 389 ISSN 0067-0049, 1538-4365 URL <https://doi.org/10.1086/190717>
- [17] Malone C M, Zingale M, Nonaka A, Almgren A S and Bell J B 2014 *ApJ* **788** 115 ISSN 0004-637X, 1538-4357 URL <https://doi.org/10.1088/0004-637x/788/2/115>
- [18] E Willcox D and Zingale M 2018 *JOSS* **3** 588 ISSN 2475-9066 URL <https://doi.org/10.21105/joss.00588>
- [19] Smith A I, Johnson E T, Chen Z, Eiden K, Willcox D E, Boyd B, Cao L, DeGrendele C J and Zingale M 2023 *The Astrophysical Journal* **947** 65 URL <https://dx.doi.org/10.3847/1538-4357/acbaff>
- [20] Guichandut S and Cumming A 2023 *Astrophysical Journal* **954** 54 (*Preprint* 2301.08769)
- [21] Almgren A, Sazo M B, Bell J, Harpole A, Katz M, Sexton J, Willcox D, Zhang W and Zingale M 2020 *Journal of Open Source Software* **5** 2513 URL <https://doi.org/10.21105/joss.02513>
- [22] Tange O 2018 *GNU Parallel 2018* (Ole Tange) ISBN 9781387509881 URL <https://doi.org/10.5281/zenodo.1146014>
- [23] Hunter J D 2007 *Comput. Sci. Eng.* **9** 90–95 ISSN 1521-9615 URL <https://doi.org/10.1109/mcse.2007.55>
- [24] Oliphant T E 2007 *Comput. Sci. Eng.* **9** 10–20 ISSN 1521-9615 URL <https://doi.org/10.1109/mcse.2007.58>
- [25] van der Walt S, Colbert S C and Varoquaux G 2011 *Comput. Sci. Eng.* **13** 22–30 ISSN 1521-9615 (*Preprint* <https://aip.scitation.org/doi/pdf/10.1109/MCSE.2011.37>) URL <https://doi.org/10.1109/mcse.2011.37>
- [26] Nethercote N and Seward J 2007 *Proceedings of the 2007 ACM SIGPLAN conference on Programming language design and implementation - PLDI '07* PLDI '07 (New York, NY, USA: ACM Press) p 89–100 ISBN 978-1-59593-633-2 URL <https://doi.org/10.1145/1250734.1250746>
- [27] Brown P N, Byrne G D and Hindmarsh A C 1989 *SIAM J. Sci. and Stat. Comput.* **10** 1038–1051 ISSN 0196-5204, 2168-3417 URL <https://doi.org/10.1137/0910062>
- [28] Turk M J, Smith B D, Oishi J S, Skory S, Skillman S W, Abel T and Norman M L 2010 *ApJS* **192** 9 ISSN 0067-0049, 1538-4365 (*Preprint* 1011.3514) URL <https://doi.org/10.1088/0067-0049/192/1/9>